Journal of Solid State Chemistry 181 (2008) 1712–1716

Contents lists available at ScienceDirect

Journal of Solid State Chemistry

journal homepage: www.elsevier.com/locate/jssc

On the composition and atomic arrangement of calcium-deficient hydroxyapatite: An ab-initio analysis

Dirk Zahn *, Oliver Hochrein

Max-Planck Institut, für Chemische Physik fester Stoffe, Nöthnitzer Str. 40, Dresden 01187, Germany

ARTICLE INFO

Article history:
Received 8 January 2008
Received in revised form
19 March 2008
Accepted 30 March 2008
Available online 4 April 2008

Keywords:
Apatite
Calcium deficiency
Defects
Biogenic calcium phosphates

ABSTRACT

A systematic study of defect constellations in calcium-deficient hydroxyapatite is reported. Along this line, we explore different arrangements for charge compensation, including cationic vacancies and substitutional defects. The overall defect constellation is governed by both the different proton affinity of the anions or energy costs related to vacancy formation and minimization of the Coulomb energy which implies small distances of the anionic and cationic defects. Depending on the type of the calcium-deficient site, this gives rise to two specific defect arrangements. Among these, the calcium ions forming triangles which embed the OH^- ions of hydroxyapatite are most likely to be deficient. The resulting charge is compensated by protonation of the OH^- ion within the deficient calcium-triangle and protonation of a PO_4^{3-} ion in the nearest neighbourhood of the vacant calcium site. The strong energetic favouring of such constellations indicates that the commonly used chemical formulae $Ca_{10-x}(HPO_4)_x(PO_4)_{6-x}(OH)_{2-x}(H_2O)_x$ $(0<x\leqslant 1)$ reflect a reasonable approximation of the composition of calcium-deficient hydroxyapatite.

1. Introduction

Apatite has attracted considerable interest in materials chemistry, mineralogy and biology. In natural apatite, in particular in apatite formed by metabolism, defects play an important role [1]. Indeed, the inorganic component of dentin and bone is represented by hydroxyapatite which is far from stoichiometric. Along this line, deficient calcium ion sites reflect a typical feature of non-stoichiometric hydroxyapatite. For calcium-deficient hydroxyapatite, the Ca/P composition ratio is known to range from 1.5 to $1.\bar{6}$ (10/6 in stoichiometric hydroxyapatite). The underlying sum formulae are commonly assumed as [2,3]

$$\text{either}\quad Ca_{10-x}(HPO_4)_x(PO_4)_{6-x}(OH)_{2-x}(H_2O)_x \tag{1.1}$$

$$\text{or}\quad Ca_{10-x}(HPO_4)_x(PO_4)_{6-x}(OH)_{2-x} \tag{1.2}$$

with $0<x\leqslant 1$.

Both compositions appear reasonable as the $-2x$ charge arising from x deficient calcium sites are compensated either by protonation of PO_4^{3-} and OH^- ions or protonation of PO_4^{3-} and removal of an OH^- ion, respectively. However, an issue which is somewhat hidden by the sum formulas of calcium-deficient hydroxyapatite as denoted above is related to the existence of two different types of calcium ions. In Fig. 1, a $1\times1\times2$ supercell of the monoclinic structure of hydroxyapatite ($x=0$) is illustrated. Therein four Ca^{2+} ions are located between the phosphate ions, while the remaining six Ca^{2+} ions are arranged as two triangles which each embed an OH^- ion. In the following, we shall use the notation Ca1 and Ca2 for distinguishing between crystallographically different calcium sites, i.e. $10\ \text{Ca} = 4\times\text{Ca1}+6\times\text{Ca2}$ for hydroxyapatite (Fig. 1).

So far it remained unclear to which ratio the two different types of calcium sites are occupied in calcium-deficient hydroxyapatite ($x>0$). This issue has important implications on the phosphate and hydroxide defects: to minimize unfavourable Coulomb interactions, it is reasonable to assume that charge neutrality is maintained as locally as possible. This implies the incorporations of the charge-compensating phosphate and/or hydroxide defects in close neighbourhood of each deficient Ca^{2+} site. Taking this as a general rule, Ca1 vacancies should be related to two protonated PO_4^{3-} ions (or one $H_2PO_4^-$ defect). Next to the Ca2 positions both OH^- and PO_4^{3-} ions can be found and OH^- vacancies as well as several possibilities of proton uptake may account for the compensation of the -2 charge of a Ca2 deficiency. On the basis of these simple considerations there hence appears to be a variety of possible defect arrangements. In particular, the strict 1:1 ratio of HPO_4^{2-} and H_2O (or OH^- vacancy) defects in the respective formulas (1.1) and (1.2) of calcium-deficient hydroxyapatite cannot be rationalized.

* Corresponding author. Fax: +49 351 4646 4002.
E-mail addresses: zahn@cpfs.mpg.de (D. Zahn), hochrein@cpfs.mpg.de (O. Hochrein).

0022-4596/$ - see front matter © 2008 Elsevier Inc. All rights reserved.
doi:10.1016/j.jssc.2008.03.035

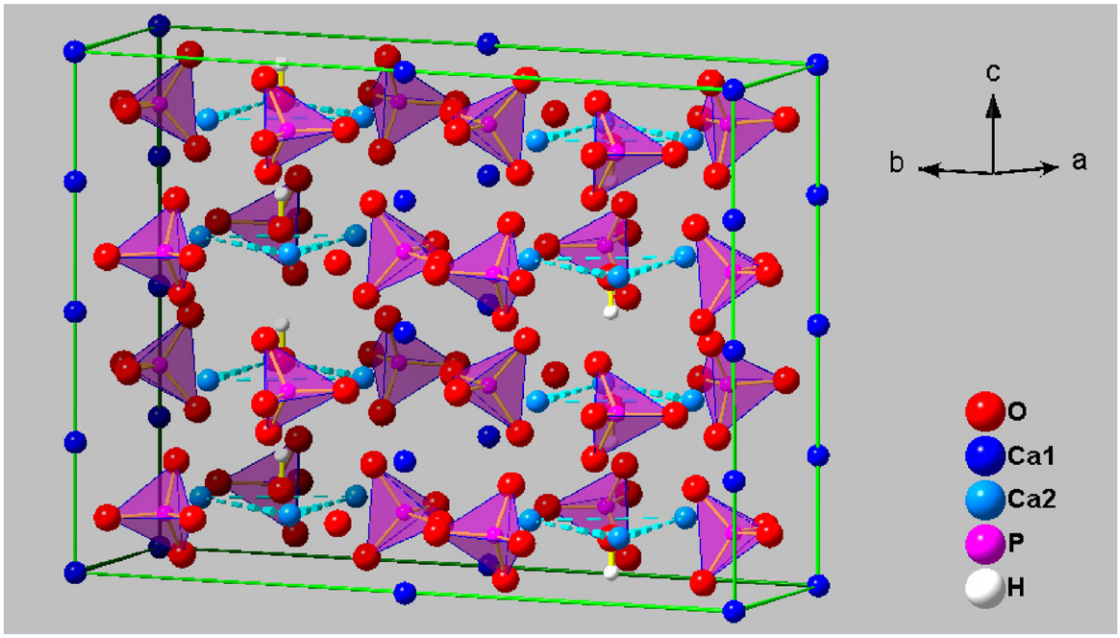

Fig. 1. Defect-free $1\times1\times2$ supercell of the monoclinic modification of hydroxyapatite as obtained from full geometry optimization. The phosphate ions are illustrated as transparent tetrahedra. Two types of calcium ions are discriminated, i.e. $Ca^{(1)}$ sites which are located between the phosphate ions and $Ca^{(2)}$ sites which form staggered triangles (dashed lines) resulting in channels parallel to the *c*-axis. Each $Ca^{(2)}$-triangle embeds a hydroxide ion.

Though diffraction experiments may resolve the atomistic structure of the bulk material; this only reflects an average over μm–mm sized or even larger samples and the direct investigation of the arrangement of single or groups of defects remains elusive. This motivated the choice of atomistic simulation approaches for exploring different defect arrangements in deficient crystals, including apatite [4–9]. Along this line, we recently presented studies of F^-, Schottky and water defects in hydroxyapatite [9]. Employing similar simulation setups we shall now address the composition and atomic configuration of calcium-deficient hydroxyapatite. To perform an unprejudiced investigation of the defect constellations, our considerations are based on the formulae:

$$Ca_{10-(x+y+z)}(HPO_4)_{2x}(PO_4)_{6-2x}(OH)_{2-2(y+z)}(H_2O)_{2z} \quad \text{with } 0<x+y+z\leqslant1 \tag{2}$$

which reflects a generalized formulation of the composition of calcium-deficient hydroxyapatite. It includes the two models 1.1 and 1.2 considered in the literature so far [2,3] and furthermore does not rely on the assumption of equal numbers of phosphate and hydroxide defects.

2. Simulation details

The starting point for the simulation systems discussed in the following is represented by a periodic model of a $1\times1\times2$ supercell of the monoclinic modification of hydroxyapatite. This model of pure hydroxyapatite was adopted from our recent study [9] which involved a full geometry optimization, i.e. relaxation of the ionic positions and the cell vectors of the simulation box by means of the same quantum mechanical approach. The relaxed structure of the $1\times1\times2$ supercell of monoclinic hydroxyapatite is illustrated in Fig. 1.

Electron structure calculations and geometry optimizations were performed using the siesta DFT package [10,11] applying the GGA functional of *Perdew*, *Burke*, *Ernzerhof* (PBE) [12]. The underlying pseudo-potentials mimicking the effect of the core electrons were created in the *Troullier–Martins* scheme [13,14] using the PBE exchange-correlation functional [12]. For the valence electrons an optimized double zeta polarization split valence basis set was chosen. Further details on the quantum mechanical setup including its verification by a series of test calculations are described in Ref. [9].

3. Results

In order to tackle the manifold of defect constellations related to calcium vacancies and local charge compensation, it is educative to first focus on the somewhat simpler case of adding a single proton to our hydroxyapatite model. Experiences obtained from such considerations are then used as starting points to the analysis of charge-neutralized models of calcium-deficient hydroxyapatite.

3.1. Proton uptake in hydroxyapatite

The system exhibits several possibilities for the uptake of protons accounting for HPO_4^{2-}or H_2O defects. To explore each case, a single proton was incorporated in the hydroxyapatite model. The respective structural optimization studies reported in the following involve refinements of the atomic positions, only. The supercell dimensions were fixed to the corresponding values of the pure hydroxyapatite model to avoid artificial expansion of the protonated systems due to the excess charge.

3.1.1. OH^- protonation

From Fig. 1 several putative H_2O defect arrangements resulting from OH^- protonation may be identified. The latter differ in terms of the orientation of the water molecule and the hydrogen bonds being formed. In monoclinic hydroxyapatite the OH^- ions are located in [0 0 1] channels embedded by triangles of calcium ions [15]. Within an $OH^-\cdots OH^-\cdots OH^-\cdots$ sequence, H_2O defects may be incorporated as $\cdots OH^-\cdots HOH\cdots OH^-\cdots$, $\cdots OH^-\cdots OH_2\cdots OH^-\cdots$ or $\cdots OH^-\cdots H_2O\cdots OH^-\cdots$ constellations. While the latter arrangement is unfavourable because of repulsive

Coulomb interactions, both the $\cdots OH^- \cdots HOH \cdots OH^- \cdots$ and the $\cdots OH^- \cdots OH_2 \cdots OH^- \cdots$ reflect favourable hydrogen bonding scenarios. Figs. 2a and b illustrate the corresponding rows of hydroxide ions and parts of the nearest neighbourhood. In the $\cdots OH^- \cdots HOH \cdots OH^- \cdots$ arrangement (Fig. 2a), one of the O–H bonds of the water molecule is directed along the *c*-axis to form a hydrogen bond to an adjacent hydroxide ion. The H–O–H angle was found as 107°. The deformation of the water molecule results from interactions with the surrounding triangle of calcium ions and a strong hydrogen bond to an adjacent phosphate group exhibiting an H⋯O distance of only 1.4 Å.

A similar hydrogen bonding situation is observed in the $\cdots OH^- \cdots OH_2 \cdots OH^- \cdots$ constellation (Fig. 2b) which is preferred by 0.18 eV over the $\cdots OH^- \cdots HOH \cdots OH^- \cdots$ arrangement. Both structures exhibit a strong $HOH \cdots OPO_3^{3-}$ hydrogen bond of relatively short H⋯O distance, whereas hydrogen bonding to the OH^- ions involves H⋯O distances of around 2.5 Å and should be considered as relatively weak. Nevertheless, the preference of the $\cdots OH^- \cdots OH_2 \cdots OH^- \cdots$ constellation may be rationalized by the alignment of the water dipole parallel to the $\cdots OH^- \cdots OH^- \cdots OH^- \cdots$ sequence.

While the monoclinic modification of apatite reflects the most stable structure at ambient conditions, natural apatite typically exhibits hexagonal symmetry. The hexagonal modification of hydroxyapatite may be obtained from the monoclinic structure via a temperature-induced order→disorder phase transition [16]. By means of molecular dynamics simulations, we recently identified the disordering of hydroxide ion orientation to involve the orientation inversion of single ions in the $\cdots OH^- \cdots OH^- \cdots OH^- \cdots$ sequences of the monoclinic structure [17]. In this arrangement, the strict alignment of dipoles within the hydroxide rows is lost.

The resulting $\cdots HO^- \cdots OH^- \cdots OH^- \cdots$ constellations may promote H_2O defect incorporation by forming an $\cdots HO^- \cdots HOH \cdots OH^- \cdots$ arrangement. The corresponding structure as obtained from energy minimization is illustrated in Fig. 2c. The total energy of this arrangement was found to be 0.41 eV larger than that of the $\cdots OH^- \cdots OH_2 \cdots OH^- \cdots$ constellation (Fig. 2b). However, the energetic cost of the orientation inversion of a hydroxide ion in our (monoclinic) model amounts to 0.33 eV. Considering the different energy levels of the two hydroxyapatite modifications, the overall costs of OH^- protonation by forming an $\cdots HO^- \cdots HOH \cdots OH^- \cdots$ arrangement of 0.41 eV in the monoclinic structure hence reduce to 0.41−0.33 = 0.08 eV in the hexagonal modification.

3.1.2. PO_4^{3-} protonation

There are two different classes of protonation sites for the phosphate ions in hydroxyapatite. The corresponding configurations may be discriminated by considering the putative nearest neighbour interactions of the proton to be added. Proton uptake in terms of HPO_4^{2-} defects opens the possibility of hydrogen bonding between adjacent phosphate ions, i.e. as $O_3POH^{2-} \cdots OPO_3^{3-}$ constellations, and hydrogen bonding to OH^- ions. Exploring both possibilities, we found $O_3POH^{2-} \cdots OH^-$ configurations to be unstable. Indeed, we observed a proton transfer leading to the formation of a water molecule. Depending on the starting configuration, the resulting H_2O defect corresponds to one of the structures shown in Figs. 2a and b.

3.2. Calcium-deficient hydroxyapatite

A profound analysis of calcium vacancies and related defect constellations for providing charge neutrality must discriminate between the two different types of calcium sites. The more complex case is surely represented by the Ca2 positions, i.e. the calcium sites forming channels of triangles which embed the hydroxide ions. However, for considering charge neutralization by proton uptake we may make use of the findings described in the previous section.

According to the observed disfavouring of phosphate protonation, we prepared a calcium-deficient hydroxyapatite model in which a Ca2 vacancy is incorporated and two protons are added to nearby hydroxide ions (Fig. 3a). However, in the course of energy minimization this starting point evolved into a different picture. While the H_2O defect placed in the deficient triangle of Ca2 sites was found to be stable, the protonation of the OH^- ion in an adjacent (and non-deficient) calcium-triangle turned out to be quite unfavourable. Indeed, energy minimization leads to a proton transfer to an adjacent phosphate ion. The latter is located in the neighbourhood of the vacant calcium site and in particular by rotation of the P–O–H bond, the excess proton is directed closer to the Ca^{2+} vacancy (Fig. 3b). Similarly, also one of the protons of the H_2O defect points towards the vacant calcium site. The missing +2 charge resulting from the removal of a calcium ion is hence compensated by proton uptake which is incorporated as locally as possible.

This tendency also applies to the incorporation of OH^- vacancies which clearly favours the removal of hydroxide ions

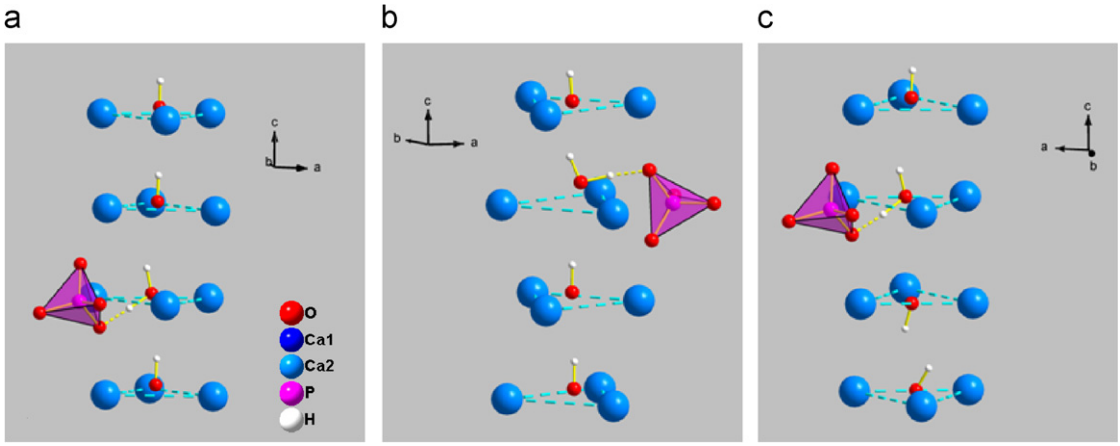

Fig. 2. H_2O defects arranged as (a) $\cdots OH^- \cdots HOH \cdots OH^- \cdots$ and (b) $\cdots OH^- \cdots OH_2 \cdots OH^- \cdots$ constellations in monoclinic hydroxyapatite. While configurations (a) and (b) result from protonation of an ordered $\cdots OH^- \cdots OH^- \cdots OH^- \cdots$ row of hydroxide ions, for the hexagonal modification also $\cdots HO^- \cdots OH^- \cdots OH^- \cdots$ constellations must be considered. Such orientation inversion may promote OH^- ion protonation by allowing (c) $\cdots HO^- \cdots HOH \cdots OH^- \cdots$ arrangements. Each configuration (a)–(c) exhibits a strong hydrogen bond to an adjacent phosphate ion with an H⋯O distance of 1.4 Å (the length of the covalent bond was found to be 1.0 Å).

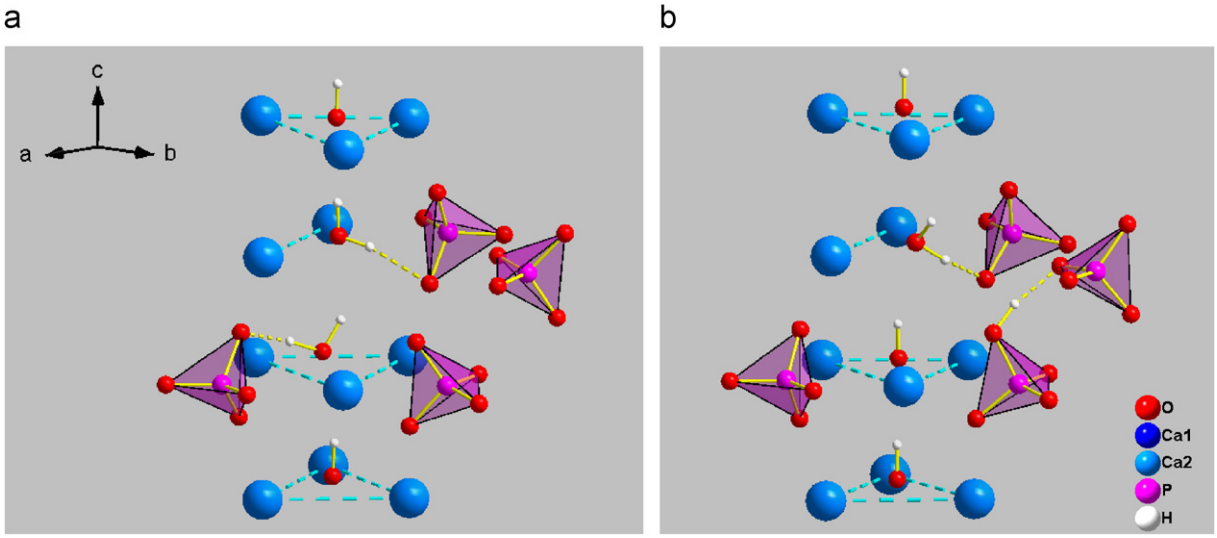

Fig. 3. $Ca^{(2)}$ vacancy and charge compensation by the uptake of two protons. The starting point (2) was chosen as two H_2O defects according to the constellations shown in Fig. 2. The structure (a) is however unstable and energy minimization leads to the arrangement (b) which exhibits a H_2O defect and a HPO_4^{2-} defect adjacent to the deficient $Ca^{(2)}$ site. The preferential defect arrangement (b) reflects a compromise of local charge compensation related to the $Ca^{(2)}$ vacancy, different proton affinities of the anions, and hydrogen bonding. The related bond lengths were found to be 1.6 and 1.7 Å for $HOH\cdots OPO_3^{3-}$ and $O_3POH^{2-}\cdots OPO_3^{3-}$ hydrogen bonds, respectively.

from deficient calcium-triangles. According to the model described above, further charge compensation was incorporated by protonation of a phosphate ion next to the vacant Ca2 site. The rectified defect constellation is illustrated in Fig. 4. Its potential energy may not directly be compared to the defect models shown in Figs. 3a and b as the number of atoms is not conserved. However, the fictitious reaction

$$\text{model 3b} \rightarrow \text{model 4} + H_2O\ \text{(vacuum)}$$

indicates a favouring of the defect arrangement illustrated in Fig. 3b by as much as 4 eV. This dramatic contrast changes only marginally when considering water association to a condensed phase rather than taking an isolated water molecule as the reference state. For example, the average energy of solvation of a water molecule in bulk water amounts to only 0.4 eV [18] and hence reduces the strong energetic disfavouring of model 4 by only 10%.

Accordingly, we expect OH^- vacancies to play only a very minor role in calcium-deficient hydroxyapatite and the chemical formulae (1.2) can be ruled out. Indeed, the only reasonable constellation corresponding to a Ca2 vacancy appears to be given by model 3b which comprises adjacent H_2O and HPO_4^{2-} defects for charge compensation. Interestingly, this arrangement exactly accounts for a composition as represented by the chemical formulae (1.1).

To complete the picture of calcium-deficient hydroxyapatite we furthermore explored the possible arrangements for incorporating a Ca1 vacancy. Each Ca1 site is located in the centre of a (deformed) octahedron formed by phosphate ions (three phosphate ions provide two oxygen atoms for Ca1 coordination, whereas three phosphate ions form only one $O\cdots Ca$ salt bridge). Accordingly, there are various possibilities of phosphate protonation which, however, upon energy minimization reduce to only two conceptionally different stable defect constellations (Fig. 5). Again, these are characterized by the systems tendency to incorporate charge compensation as locally as possible. The most favoured arrangement corresponds to two HPO_4^{2-} defects in a constellation which allow directing the protons closest to the deficient Ca1 site (Fig. 5b).

With respect to the *c*-axis, accumulation of two protons in a triangle of phosphate ions above or below the vacant Ca1 site is possible (Figs. 5a and b). The small disfavouring by 0.08 eV of the two constellations 5a and 5b may be rationalized by the formation

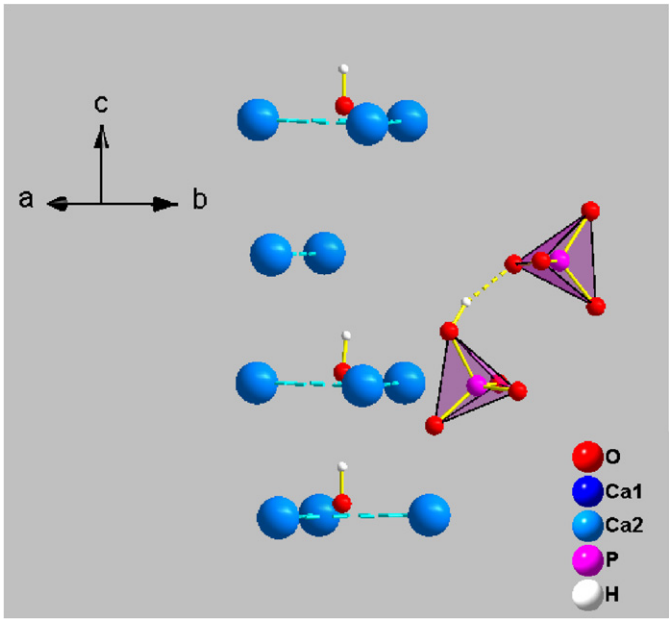

Fig. 4. $Ca^{(2)}$ vacancy and charge compensation by incorporation of an OH^- vacancy and a HPO_4^{2-} defect adjacent to the deficient calcium site. Our calculations indicate a clear disfavouring of OH^- vacancies compared to proton uptake as illustrated in Fig. 3.

of a net dipole moment resulting from incorporating both protons below(above) the deficient Ca1 position. Dihydrogenphosphate ions were found to be unstable and undergo proton transfer to form two monohydrogenphosphate ions. Comparing the potential energy levels of the optimized defects arrangement around Ca1 and Ca2 vacancies indicates that the latter type of calcium vacancies are preferred by 0.7–0.8 eV.

4. Conclusion

While crystal growth represents a non-equilibrium process which may trap energetically less preferred constellations, it is

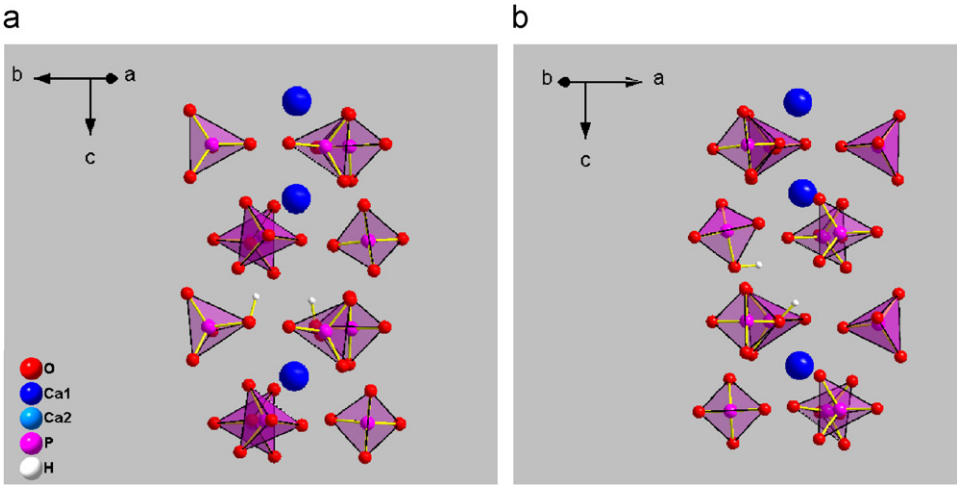

Fig. 5. $Ca^{(1)}$ vacancy and charge compensation by incorporation of two HPO_4^{2-} defects adjacent to the deficient calcium site. Two types of stable constellations were identified of which configuration (b) exhibits the lowest potential energy. However, the latter is nevertheless disfavoured over the preferential defect arrangement related to $Ca^{(2)}$ vacancies by 0.7 eV.

nevertheless reasonable to assume the majority of calcium vacancies in calcium-deficient hydroxyapatite to correspond to the most favourable structure identified from our simulations. The structural optimization studies on various arrangements of calcium-deficient hydroxyapatite revealed a clear preference of Ca2 vacancies accompanied by charge neutralization by adjacent H_2O and HPO_4^{2-} defects displaying an exact 1:1 ratio. Ca1 vacancies were found to be disfavoured by a minimum of 0.7 eV. Strikingly, the preferential constellation identified from our calculations accounts for a composition as represented by the widely assumed chemical formulae $Ca_{10-x}(HPO_4)_x(PO_4)_{6-x}(OH)_{2-x}(H_2O)_x$ with $0<x\leqslant 1$.

Accordingly, the incorporation of calcium vacancies may account for a depletion of OH^- ions by up to 50%. From solid-state NMR spectroscopy experiments, natural bone was found to contain only about 20% of the OH^- ions present in pure hydroxyapatite [19]. We suggest that this difference is mainly attributed to hydroxide substitution by carbonate ions. The latter species accounts for 3–8 wt% in biogenic apatite [1].

References

[1] S.V. Dorozhkin, M. Epple, Angew. Chem. 114 (2002) 3260.
[2] R.Z. LeGeros, G. Bonel, R. Legros, Calcif. Tissue Res. 26 (1978) 111.
[3] J.C. Elliot, Structure and Chemistry of the Apatites and other Calcium Orthophosphates in Studies in Inorganic Chemistry 18, Elsevier, Amsterdam, 1994.
[4] R. Kniep, P. Simon, Top. Curr. Chem. 270 (2006) 73.
[5] D. Zahn, O. Hochrein, A. Kawska, J. Brickmann, R.J. Kniep, Mater. Sci. 42 (2007) 8966.
[6] P. Regnier, A.C. Lasaga, R.A. Berner, O.H. Han, K.W. Zilm, Am. Mineral. 79 (1994) 809.
[7] P. Rulis, L. Ouyang, W.Y. Ching, Phys. Rev. B 70 (2004) 155104.
[8] R. Astala, M.J. Stott, Chem. Mater. 17 (2005) 4125.
[9] D. Zahn, O. Hochrein, Z. Anorg. Allg. Chem. 632 (2006) 79.
[10] P. Ordejon, E. Artacho, J.M. Soler, Phys. Rev. B 53 (1996) 10441.
[11] J.M. Soler, E. Artacho, J.D. Gale, A. Garcia, J. Junquera, P. Ordejon, D.J. Sanchez-Portal, Phys.: Condens. Matter 14 (2002) 2745.
[12] J.P. Perdew, K. Burke, M. Ernzerhof, Phys. Rev. Lett. 77 (1996) 3865.
[13] N. Troullier, J.L. Martins, Phys. Rev. B 43 (1991) 1993.
[14] N. Troullier, J.L. Martins, Phys. Rev. B 43 (1991) 8861.
[15] J.C. Elliott, P.E. Mackie, R.A. Young, Science 180 (1973) 1055–1057.
[16] M.I. Kay, R.A. Young, A.S. Posner, Nature 204 (1964) 1050–1052.
[17] O. Hochrein, R. Kniep, D. Zahn, Chem. Mater. 17 (2005) 1978.
[18] D. Zahn, B. Schilling, S.M. Kast, J. Chem. Phys. B 106 (2002) 10725.
[19] G. Cho, Y. Wu, J.L. Ackerman, Science 300 (2003) 1123.